Thermodynamics of phase transitions in Zintl clusters from density functional theory: making and breaking of bonds in Ba_3Ge_4.

Yao Zhao and John E. McGrady
Department of Chemistry, University of Oxford,
South Parks Road,
Oxford,
OX1 3QR,
United Kingdom

Contents

1 Thermal expansions of Ba_3Ge_4 in the QHA approximation

The stacked curves on the left of Figure S1 show the variation in Helmholtz Free energy computed at a range of temperatures for cells optimised subject to the constraint of fixed volume. The red line in each Figure passes through the minimum energy volume at each temperature, and the variation in optimised volume as a function of temperature is shown in the middle plot. The third plot shows the thermal expansion as a percentage of the original volume. All values are for a unit cell containing four formula units.

(a) tetragonal

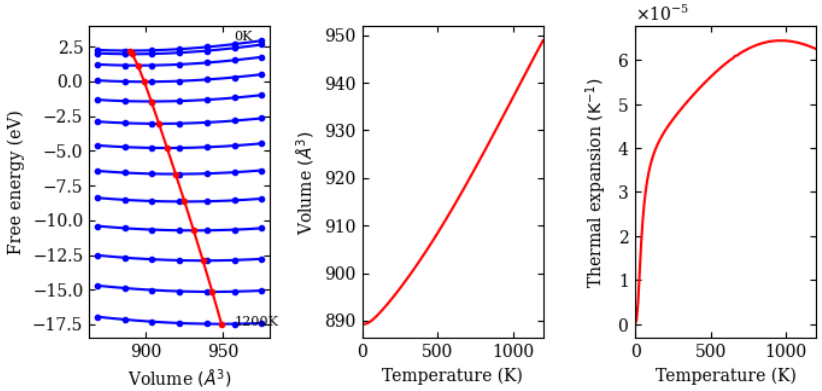

(b) orthorhombic

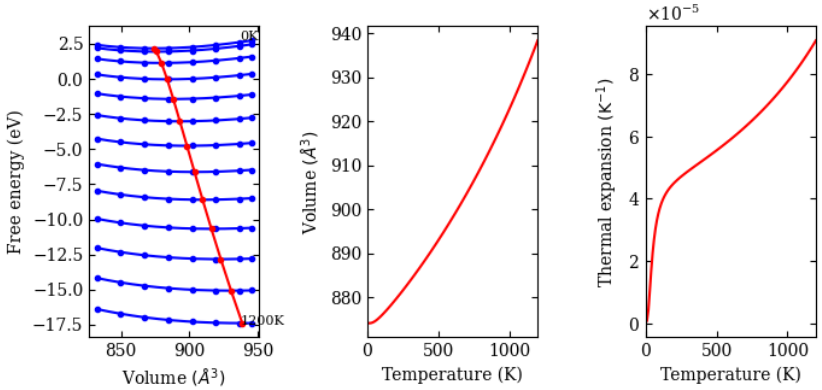

(c) p-tetragonal

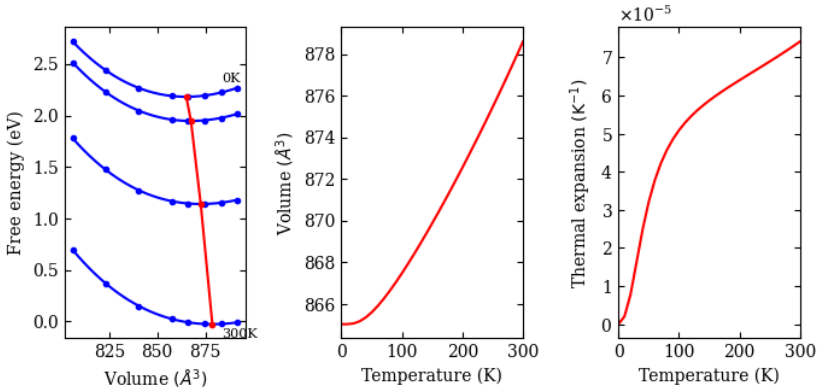

Figure S1 Summary of thermal expansions of Ba_3Ge_4 phases predicted by QHA.

Figure S2, below, collects together the thermal expansion coefficients, α, for the three phases shown in the right-hand panels of Figure S1. The tetragonal and orthorhombic phases are closely aligned and approximately linear between 70 and 600 K. The p-tetragonal phase, in contrast, expands more rapidly with temperature and the plot becomes distinctly non-linear beyond ∼300 K. This inflection point marks the onset of dynamic instability, and hence the breakdown of the QHA. For this reason, we do not report thermodynamic parameters for the p-tetragonal phase beyond this temperature.

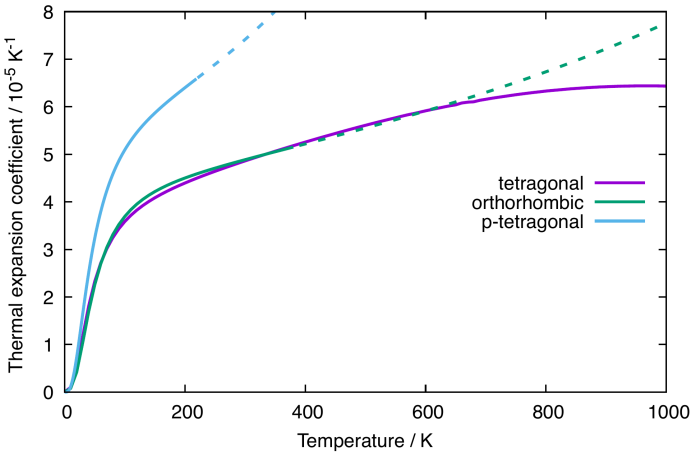

Figure S2 Comparison of temperature dependencies of thermal expansion coefficients of Ba_3Ge_4 at ambient pressure. The transition from full to dashed lines indicates the point where when the $\left[\frac{d^2\alpha}{dT^2}\right]_p \geq 0$. Beyond this point, the validity of the QHA is uncertain according to criteria set out by Wentzcovitch *et al.*.[1,2]. The thermal expansion coefficients for the p-tetragonal phase diverge markedly at ∼400 K and the Gibbs free energy is therefore truncated beyond 300 K in this study. The orthorhombic phase shows only minor signs of divergence above ∼1000 K and $\left[\frac{d^2\alpha}{dT^2}\right]_p \leq 0$ for the the tetragonal phase at all temperatures below the melting point.

2 Phonon modes of Ba_3Si_4

In the main text, the phonon band structure and density of states was discussed in detail for Ba_3Ge_4. The corresponding data for Ba_3Si_4 are shown in Figure S3, below. The key difference is that the lighter Si atoms lead to higher frequency phonon modes for the internal stretches of the Si_4 units, and hence to a cleaner distinction between them and the ion-ion modes.

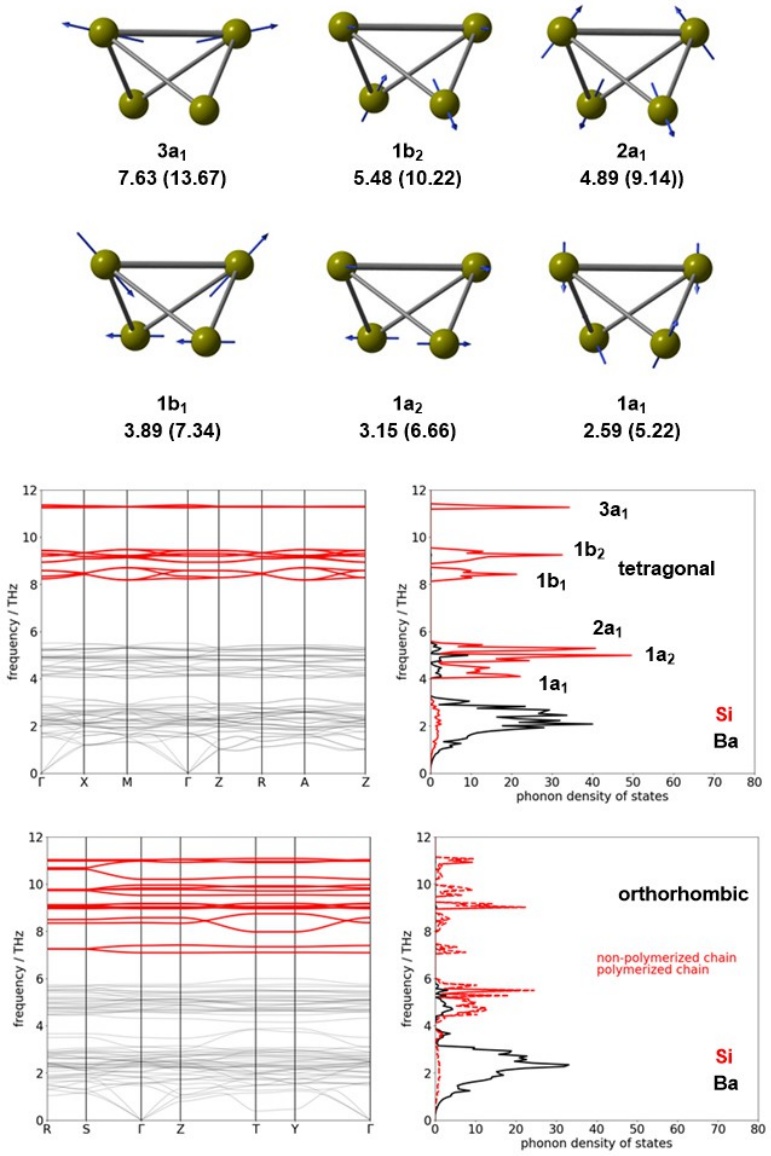

Figure S3 Phonon modes for Ba_3Si_4 in the tetragonal and orthorhombic structures. Note that the p-tetragonal phase was not located.

3 Bader charge analysis

In analysing the changes in phonon dispersion curves in the α and β phases, we have argued that it is the change in volume of the unit cell, and with it the decreased distance between the ions, that drives the change in entropy. Implicit in this is that the changes in electronic structure associated with the transition are negligible. To evaluate this point, we show in Table S1 the Bader atomic charge calculated within optB86b-vdW. Atoms are labelled according to their Wycoff positions and the multiplicities in the unit cell. Atoms 8q and 8n in the orthorhombic phase are those in the polymerised clusters while 8p and 8o are in the non-polymerised clusters. It can be seen that the change in ionic charge through the phase transitions is very minor.

Table S1 Bader charge analysis of Ba_3Ge and Ba_3Si_4 (optB86b-vdW).

	Ba_3Ge_4						Ba_3Si_4			
atom	tetragonal		orthorhombic		p-tetragonal		tetragonal		orthorhombic	
Ba	4e	1.09	4k	1.08	4e	1.10	4e	1.10	4k	1.07
			4l	1.11					4l	1.11
	4d	1.14	8m	1.11	4d	1.10	4d	1.14	8m	1.10
	4g	1.15	4g	1.11	4g	1.11	4g	1.16	4g	1.11
			4j	1.13					4j	1.12
Ge,Si	8i	-0.67	8q	-0.67	8i	-0.67	8i	-0.69	8q	-0.72
			8p	-0.67					8p	-0.70
	8j	-1.02	8n	-0.96	8j	-0.98	8j	-1.01	8n	-0.86
			8o	-1.03					8o	-1.03

Notes and references

[1] R. M. Wentzcovitch, B. B. Karki, M. Cococcioni and S. de Gironcoli, *Phys. Rev. Lett.*, 2004, **92**, 018501.

[2] J. Tsuchiya, T. Tsuchiya and R. M. Wentzcovitch, *Journal of Geophysical Research: Solid Earth*, 2005, **110**, B02204.